frontiers | Frontiers in Energy Research

TYPE Original Research
PUBLISHED 09 April 2024
DOI 10.3389/fenrg.2024.1357459

OPEN ACCESS

EDITED BY
Shuqing Zhang,
Tsinghua University, China

REVIEWED BY
Haibo Li,
Tsinghua University, China
Can Ding,
China Three Gorges University, China

*CORRESPONDENCE
Chongbin Huang,
leeyen5983@163.com

RECEIVED 18 December 2023
ACCEPTED 25 March 2024
PUBLISHED 09 April 2024

CITATION
Huang C, He H, Wang Y, Miao R, Ke Z and Chen K (2024), Low-voltage characteristic voltage based fault distance estimation method of distribution network.
Front. Energy Res. 12:1357459.
doi: 10.3389/fenrg.2024.1357459

Low-voltage characteristic voltage based fault distance estimation method of distribution network

Chongbin Huang*, Haipeng He, Ying Wang, Rixian Miao, Zhouzhi Ke and Kai Chen

Zhanjiang Power Supply Bureau of Guangdong Power Grid Co., Ltd., Zhanjiang, China

The traditional medium-voltage distribution network fault location method uses mainly the voltage and current measurements of the medium-voltage side, which results in problems such as high installation costs at the measuring points and complicated postoperation and maintenance work. Therefore, a fault location idea based on the distributed measurement of low-voltage side voltage is proposed in this paper. First, the characteristic voltage is adaptively selected according to the fault type. Second, the suspected fault section is determined by comparing the characteristic voltage amplitude of each measuring point. Third, the fault section is located using the section unit characteristic voltage drop defined for each suspected fault section. Finally, fault distance estimation is achieved based on the voltage difference matrix and characteristic voltage analysis. This method achieves accurate fault distance identification based on the distribution difference of the characteristic voltage of the low-voltage side under the fault state. This work provides a new economical and practical idea for determining the fault locations of distribution networks. The effectiveness of this method is evaluated by considering a 10 kV distribution network in Guangdong Province built in PSCAD/EMTDC.

KEYWORDS

distribution network, fault section location, fault distance estimation, distributed measurement, characteristic voltage of low-voltage

1 Introduction

As a key component linking the power system to terminal users, the operational reliability of the medium-voltage distribution network is critical. However, due to the complex operating environment and wide distribution of medium-voltage distribution networks, it is difficult to avoid faults. According to statistics, approximately 90% of customer outages are caused by distribution network faults (Bingyin et al., 2017). Therefore, the fast and accurate fault location of distribution networks after a fault is highly important for rapidly reducing outage times and losses and improving the reliability of the power supply to the grid.

Many studies have been conducted on fault locations in medium-voltage distribution networks. According to differences in the principle and measurement points, the methods can be divided into impedance methods based on station-side voltage/current measurements, travelling wave methods based on station-side or multipoint travelling wave signal measurements, and distributed multipoint measurement methods. Among

these methods, the impedance method (Rong et al., 2013; Lu et al., 2016; Gabr et al., 2017) and the travelling wave method (Shichao and Liu, 2010; Rui et al., 2014; Feng et al., 2021) are traditional location methods that have been effectively applied for determining fault locations in transmission networks. However, when locating faults in distribution networks, the impedance method fails to completely solve the location problems caused by diverse line types and many branches; the travelling wave method faces problems such as difficulty identifying wave head signals caused by short distribution lines and complex structures; and practical application challenges such as high sampling frequency and costly equipment investments also arise.

In recent years, with the ubiquity and diversification of measuring device types, additional data sources have been provided for determining fault locations in distribution networks. To overcome the fault location difficulties associated with the complexity of distribution network structures, positioning methods based on distributed multipoint measurements, also known as wide-area communication methods, have become popular research topics (Feng et al., 2017; GE et al., 2020; Jia et al., 2020). Measurement objects usually include feeder currents and node voltages; synchronous phase-based measurements have also been applied in fault locations in distribution networks (Li et al., 2020; Zhang et al., 2020; Yang B. et al., 2022). Fault position methods based on feeder current measurements utilize the basic principles of distribution network automation and fault indicators, achieving positioning accuracies proportional to the number of monitoring terminals; this type of method requires the installation of a current measurement device on the feeder, incurring a large installation, operation and maintenance workload. Fault position methods based on node voltage measurements are usually performed at the locations of subsection posts, ring main units, distribution transformers, etc., to achieve sparse measuring positioning based on medium-voltage-side voltages. Currently, for multipoint measurement locations, introducing a current injection source at the fault point is common (Dobakhshari and Ranjbar, 2015; Feng and Abur, 2016; Dobakhshari, 2018; Jia et al., 2019; Sun et al., 2020), and voltage data from sparse measurement points and the node impedance matrix are used to calculate the node injection current to obtain the fault section. In (Trindade and Freitas, 2017), pseudo fault points were excluded by establishing a low-voltage zone through sparse measurement point data based on multiple fault points derived from the impedance method. (Yan et al., 2021). improved upon the relevant parameters on this basis, increasing the accuracy of the location results. The direct voltage matching method can also be used for multipoint measurements (Lotfifard et al., 2011; Buzo et al., 2021), but fault simulation must be performed at all nodes, which requires high grid modelling accuracy. Guaranteeing accuracy while estimating fault resistance through an iterative method is complicated. In (Alwash et al., 2015), the authors used the zero reactive power consumption of resistive faults to establish a correlating equation to obtain the fault distance; however, pseudo fault points may be obtained by this method and need to be further eliminated. In (Trindade et al., 2014), the short-circuit current was calculated during faults at all nodes using the voltage at the measurement point, and the fault location was determined with the principle of minimum current error; however, this method also produces pseudo fault points.

Existing fault position methods based on multipoint voltage measurement are mainly based on medium voltage side measurement. The medium voltage side voltage can reflect the fault information more intuitively and accurately, but the medium voltage side measurement needs to be installed with a voltage transformer at the same time, which may bring the risk of ferromagnetic resonance to the system while increasing the cost. For this purpose, a practical solution has been provided for fault location in distribution networks based on low-voltage side measurements.

In (Jia et al., 2015), the amount of negative sequence voltage change at each measurement point on the low-voltage side is determined before and after the fault, and the group with the maximum amount is used to determine the fault location. However, this method may lead to misjudgement when some branch circuits are longer, and it cannot be used for locating three-phase ground faults due to the use of a single negative sequence voltage as the object of analysis. Most of the existing fault locations based on low-voltage measurement points use a negative sequence component; however, using only this feature quantity cannot yield the three-phase fault location or the best location effect under the insensitive working conditions of the negative sequence feature quantity, while different feature quantities have different sensitivities to the fault types.

To adapt to the complex structure of distribution networks, fault distance estimation relies mainly on the distributed measurement method. However, as the number of distribution network branches increases, the number of measurement points needed for positioning also increases. Too many measuring points will lead to high costs, and synchronizing data among multiple measuring points is also difficult. A fault distance estimation method based on wide-area communication was proposed in the literature (Arsoniadis et al., 2021; Tashakkori et al., 2021; Crespo and Moreto, 2022; Yang R. et al., 2022; Conte et al., 2023; Dashtdar et al., 2023). However, for complex and large power grids, a large number of measuring points need to be arranged, which leads to a high cost of positioning, and data synchronization between a large number of measuring points is difficult to address. In addition, with increases in city size and the construction of energy infrastructure, an increasing number of cities are constructing underground cables to replace overhead cables considering environmental and safety concerns. Under fault conditions, an underground cable causes a large amount of distributed capacitor current to return to the distribution network, which affects the accuracy of the fault location. References (Buzo et al., 2021; Penido et al., 2022) proposed fault distance estimation methods for active distribution networks based on wide area communication methods but did not consider the line capacitance effect on the ground. Reference (Li et al., 2021) considered the capacitance effect of a line to the ground but ignored the influence of the load branch. For some two-terminal positioning methods (Crespo and Moreto, 2022), only the faults occurring on the main feeder can be located, and the faults on the branch cannot be located. In summary, the distributed measurement method based on the information of the medium-voltage side requires a large number of measurement points to achieve fault distance estimation, which leads to high costs. Moreover, because distribution network automation has not been sufficiently developed and distribution network

measurement devices do not have phasor measurement conditions, accurate fault distance estimation is difficult.

In this paper, aiming at the above problems, the impacts of different types of faults on the low-voltage side are found to be quite different through analysing the voltage distribution characteristics of the medium-voltage side and the voltage transmission characteristics of the distribution transformer when the distribution network is faulty. For this reason, the characteristic voltages of different fault types are determined according to the fault distribution characteristics of each voltage quantity on the low-voltage side. The characteristic voltages are used to determine the fault paths and combined with the fault section search algorithm to avoid misjudgement of fault sections, achieving the fault section location of the medium-voltage distribution network based on the characteristic voltage measurements of the low-voltage side. In addition, a new fault distance estimation method based on a voltage difference matrix and characteristic voltage analysis is adopted that incorporates the information of the low-voltage side to achieve fault distance measurement. The inductance effect and capacitance effect of actual distribution network lines are also considered in this paper; thus, the distributed parameter model of distribution network lines is adopted. This method improves the positioning method of multipoint measurements and greatly reduces the number of measuring points needed for positioning.

2 Analysis of fault voltage distribution characteristics

When a fault occurs on the medium-voltage side of the distribution network, the voltage at the fault point significantly decreases, and the voltage amplitude of the entire grid changes to a certain extent; thus, the fault location in the distribution network can be determined by using the distribution characteristics of the system voltage. Due to the transformer transmission characteristics, the measured information on the low-voltage side indirectly reflects the voltage information on the medium-voltage side; however, due to the limitations of the distribution transformer connection, the fault information on the medium-voltage side cannot be completely transferred to the low-voltage side. For this reason, in this section, on the basis of analysing the distribution characteristics of the medium-voltage side voltage in the entire network during faults, the transmission characteristics of the distribution transformer are considered to analyse the distribution law of the low-voltage side measured voltage under different fault types.

2.1 Fault voltage distribution characteristic of medium voltage side

Upstream of the fault point, because of the large fault current flowing from the system power side to the fault point, the positive sequence voltage magnitude decreases gradually. Only load currents flow on the branch circuits (nonfault paths); therefore, the branch voltage magnitude changes are small. The positive sequence voltage amplitude downstream of the fault point is then close to that at the fault point. In addition, the load current is low, so the voltage drops slightly. The distribution characteristics of the negative-sequence voltage and zero-sequence voltage in the fault path are opposite to those of the positive-sequence voltage. The amplitudes of the negative sequence voltage and zero sequence voltage from the power supply terminal to the point of failure gradually increase and approach the maximum value at the point of fault. The amplitude downstream is close to that of the fault point.

It should be noted that the difference in voltage distributions in the network is essentially due to the voltage drop generated by the current on the line. Although the sequence voltage distribution characteristics are generally the same for different fault types, the sequence current levels under different fault types are very different, so the voltage distribution characteristics in the network also differ for different fault types.

Unlike the analysis of the sequence voltage, where complete decoupling between positive, negative, and zero sequence circuits can be achieved, the distribution characteristics of phase and line voltages are more complex. To simplify the analysis, only the faulted phase voltage and the line voltage associated with the faulted phase are analysed in this article. The fault phase voltage gradually decreases from the power side of the system through the fault point to the end of the line downstream of the fault. The voltage change per unit line length downstream of the fault is extremely small, and the distribution law is nearly the same as that of the positive sequence voltage. The speed of change in the voltage on the line is positively correlated with the current amplitude. The distribution law of the line voltage variation is directly related to the system's neutral grounding method and fault type. For single-phase grounding faults in small-current grounding systems, each line voltage on the low-voltage side is almost unaffected; for single-phase grounding faults in small-resistance grounding systems, the line voltage gradually decreases from the power supply terminal to the point of fault; for interphase short-circuit faults, the line voltage gradually decreases to zero from the power supply terminal to the point of fault, and the downstream side of the fault is close to the fault point.

2.2 Influence of the distribution transformer on the voltage-characteristics of the low voltage side

With the purpose of further obtaining the change characteristics and distribution law of low-voltage side voltages under different fault conditions, the low-voltage side voltage characteristics are analysed in conjunction with the operating characteristics of distribution transformers in this paper. Our 10/0.4 kV distribution transformer mainly uses Dyn11 and Yyn0, two kinds of linkages (Xu et al., 2019). Here, we take the typical linkage Dyn11 as an example to reveal the transmission law of each voltage quantity through the transformer. According to the transformer's transfer characteristics, the phase voltage on the low-voltage side can be expressed as:

$$\begin{bmatrix} U_{\mathrm{a}}^{'} \\ U_{\mathrm{b}}^{'} \\ U_{\mathrm{c}}^{'} \end{bmatrix} = \frac{1}{\sqrt{3}K} \begin{bmatrix} 1 & -1 & 0 \\ 0 & 1 & -1 \\ -1 & 0 & 1 \end{bmatrix} \begin{bmatrix} U_{\mathrm{a}} \\ U_{\mathrm{b}} \\ U_{\mathrm{c}} \end{bmatrix} \tag{1}$$

where U_{a}, U_b, and U_c denote the phase voltage of the primary side (medium-voltage side); $U_a^{'}$ and $U_b^{'}$; $U_c^{'}$ denote the phase voltage of the secondary side (low-voltage side); and K denotes the

transformation ratio. The relation equation shows that the phase voltage of the low-voltage side corresponds to the line voltage of the medium-voltage side. Furthermore, the low-voltage side line voltage may be expressed as:

$$\begin{bmatrix} U'_{ab} \\ U'_{bc} \\ U'_{ca} \end{bmatrix} = \frac{1}{\sqrt{3}K} \begin{bmatrix} 1 & -2 & 1 \\ 1 & 1 & -2 \\ -2 & 1 & 1 \end{bmatrix} \begin{bmatrix} U_a \\ U_b \\ U_c \end{bmatrix} \tag{2}$$

where U'_{ab}, U'_{bc}, and U'_{ca}indicate the secondary side line voltage. Compared with Formula (1), the low-voltage side line voltage is still a linear transformation of the phase voltage of the MV side, but the relationship is more complex.

To further analyse the rule of law of the sequence voltage, so that the medium-voltage side is positive, negative, and zero for U_1, U_2, and U_0 and the corresponding low-voltage side sequence components for U'_1, U'_2, and U'_0, respectively; then, the corresponding medium- and low-voltage side sequence components are:

$$\begin{bmatrix} U'_1 \\ U'_2 \\ U'_0 \end{bmatrix} = \frac{1}{K} \begin{bmatrix} e^{30°j} & 0 & 0 \\ 0 & e^{-30°j} & 0 \\ 0 & 0 & 0 \end{bmatrix} \begin{bmatrix} U_1 \\ U_2 \\ U_0 \end{bmatrix} \tag{3}$$

It can be seen from the formula that the zero sequence voltage cannot be transferred to the low voltage side through the distribution transformer. The positive and negative sequence voltages have shifted phases, and the amplitudes decrease according to the ratio when they are transferred.

In this paper, the IEEE34 node system is taken as an example. The fault sequence voltage components are calculated according to the symmetric component method, and the phase voltage and line voltage magnitudes are subsequently obtained. The neutral ungrounded system and the neutral directly grounded system are two extreme cases, and the voltage changes can be calculated directly. Small resistance grounding and resonant grounding systems are affected by system parameters and the size of the neutral grounding impedance (arcing coil, resistance), which makes it difficult to accurately calculate the amount of each voltage change. Therefore, assuming the fully compensated state of the arcing coil in the resonant grounding system, the voltage variations are the same as those in the ungrounded system, while the small resistance grounding system is affected by the distance of the fault, and the voltage variations fall between the directly grounded and the ungrounded system. It should be noted that in the above analysis, only the voltage change rule of the 10 kV side of the distribution network is considered. Due to the influence of the distribution transformer, the medium-voltage side of the sequence voltage information cannot be completely reflected to the low-voltage side, and the low-voltage side of the voltage change needs to be analysed in conjunction with the distribution transformer. According to the transfer matrix for each voltage, the line voltage on the medium-voltage side corresponds to the phase voltage on the low-voltage side; thus, the changes of the two are synchronized. For the sequence component, the zero sequence cannot pass through the transformer; instead, the positive and negative sequence components pass through the transformer in the amplitude and phase of the corresponding changes, but both sides of the amplitude in the change are also kept in sync. The low-voltage changes in the voltage side are shown in Table 1, as calculated using Formulas (1)-(3). Take the single-phase grounding fault and the neutral point directly grounded as an example. The positive sequence voltage of phase A $V_1 = \left(1 - \frac{Z_{1\Sigma}}{3R_f + 2Z_{1\Sigma} + Z_{0\Sigma}}\right)E_1$, combined with $Z_\Sigma^0 = 3Z_\Sigma^+$, $R_f = 0$ and Formulas (3), it can be concluded that the maximum change of positive sequence voltage on the low voltage side is 0.2p.u. The same is true for other voltage characteristics.

3 The method of fault section location

3.1 Theory of fault section location

According to the analysis of the fault distribution characteristics in the first segment, the variation ranges of the voltages on the medium-voltage side and low-voltage side are different for different fault types. To achieve fault location based on the fault distribution characteristics on the low-voltage side, the voltage characteristic with the maximum distribution difference is selected as the characteristic voltage. For example, when a single-phase fault occurs, the negative sequence component of the fault point reaches the maximum value of the whole distribution network; thus, the fault section can be confirmed by determining the maximum value of the negative sequence component. Additionally, the positions of faults can be confirmed by determining the minimum value of the phase voltage or the maximum value of the negative sequence voltage. The characteristic voltages adapted to different types of faults are obtained by the data analysis method in the following segment. The measuring points fail to obtain the value of the characteristic voltage directly in most cases, and the measured extreme value of the fault voltage typically corresponds to the location downstream of the fault. In other words, faults are located in the path between the transformer substation and the measuring point corresponding to the extreme value of the characteristic voltage. Once this path is determined, the characteristics of the current difference between the upstream and downstream currents of the fault can be used to search for the fault, and the specific fault section can be determined by using relevant algorithms.

3.2 Characteristic voltage determination

To determine the fault section location using the distribution character of the characteristic voltage on the low-voltage side, two conditions should be met as follows: 1) the characteristic voltage at the fault point must have amplitude characteristics that are different from those of the rest of the distribution network, such as maximum or minimum values; and 2) the distribution character of the characteristic voltage at the fault point should obviously differ upstream and downstream of the fault point.

The voltage must also be easily measured. Based on these conditions, the voltages on the low-voltage side under the different types of faults in Table 1 are analysed. Only the negative sequence voltage meets the two conditions given a single-phase grounding fault; both the negative sequence voltage and phase voltage meet the conditions under the circumstances of a phase-to-phase short circuit and two-phase ground short circuit;

TABLE 1 Voltage variation of low voltage side at fault point under different faults.

Fault type	Voltage type	Voltage variation (p.u.)		
		Direct grounding	Small resistance grounding (10Ω)	Ungrounding and resonant grounding
LG	Positive Sequence	0.2	0~0.2	0
	Negative Sequence	0.2	0~0.2	0
	Zero Sequence	0	0	0
	Phase Voltage	0.28	0~0.28	0
	Line Voltage	0.08	0~0.08	0
LL	Positive Sequence	0.5	0.5	0.5
	Negative Sequence	0.5	0.5	0.5
	Zero Sequence	0	0	0
	Phase Voltage	1	1	1
	Line Voltage	0.5	0.5	0.5
LLG	Positive Sequence	0.57	0.5~0.57	0.5
	Negative Sequence	0.43	0.43~0.5	0.5
	Zero Sequence	0.43	0~0.43	0.5
	Phase Voltage	1	1	1
	Line Voltage	0.57	0.5~0.57	0.5
3L	Positive Sequence	1	1	1
	Negative Sequence	0	0	0
	Zero Sequence	0	0	0
	Phase Voltage	1	1	1
	Line Voltage	1	1	1

TABLE 2 Determination of characteristic voltage.

Transformer connection mode	Single-phase ground fault	Phase-to-phase fault and two-phase ground fault	Three-phase ground fault
Dyn11	negative sequence	negative sequence	any phase voltage
Yyn0	negative sequence	negative sequence	any phase voltage

and both the line voltage and phase voltage meet the conditions under the circumstance of a three-phase fault. Considering the influence of the connection mode of the distribution transformer on the characteristic voltage, combined with the actual situation in which the distribution transformer mainly adopts the Dyn11 and Yyn0 connection modes, the characteristic voltage selection of the low-voltage side is shown in Table 2. When locating a single-phase fault in an actual distribution network, the characteristic negative sequence voltage should be varied before and after the fault to eliminate the negative sequence component introduced by the three-phase imbalance in the distribution network. Compared with the direct use of electricity to locate the fault, this method needs to judge the fault type in advance and takes more time. Fault location is often used for post-fault estimation of permanent faults, it does not require real-time estimation like relay protection, so the time taken to determine the fault type is acceptable. In addition, compared with the direct use of electrical parameters, using characteristic voltage for fault location can locate the fault section more directly and accurately.

3.3 The suspected fault path determination and section division

With the maximum value of the characteristic voltage at the fault point, the characteristic voltage amplitude is obtained according to each measuring point, and the maximum or minimum point of the characteristic voltage is selected. It can be preliminarily determined

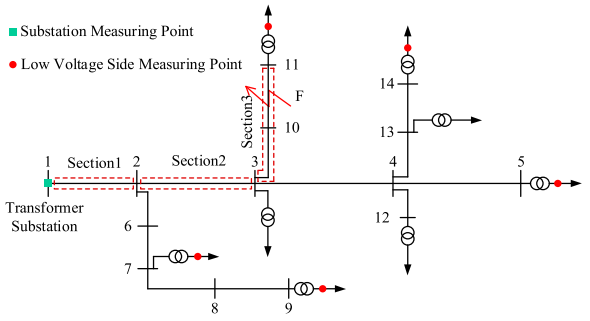

FIGURE 1
Schematic diagram of distribution fault location.

that the fault point is between the main station and the measuring point with the maximum characteristic voltage, and the path is defined as the suspected fault path. A fault may occur in any segment of the path. In the simple distribution network topology shown in Figure 1, the voltage measurement points are configured on the low-voltage side of the substation and at the end of each long branch (nodes 5, 7, 9, 11 and 14). Assuming that a single-phase ground fault occurs at F in the figure, the characteristic voltage amplitudes of low-voltage points at nodes 5, 7, 9, 11, and 14 are collected and compared. The amplitude of the characteristic voltage (negative sequence voltage) is the largest on the low-voltage side of node 11. The path between nodes 1 and 11 is identified as the suspected fault path, and the path is divided into several sections according to the branches with measuring points. There are low-voltage measurement points at the ends of the branches corresponding to nodes 2 and 3. Therefore, the suspected fault path can be divided into three subsegments and labelled, as shown in the dashed box in Figure 1.

In practical applications, considering the measurement error of the equipment, the difference in the characteristic voltages between the fault point and its downstream branch measuring point may be small, and multiple measuring points with the same maximum or minimum voltage amplitude may exist. In this case, the path between the first common node of these measurement points and the substation should be identified as the suspected fault path.

3.4 Fault section searching algorithm

The difference in the characteristic voltage distributions in the power network is essentially the voltage drop caused by the corresponding characteristic current. The larger the corresponding characteristic current is, the more convenient the method is for determining the fault location. Due to the large difference between the characteristic current upstream and downstream of the fault, the characteristic current can be calculated using this approach to determine the fault section. The suspected fault path (nodes 1–11) and the low-voltage side characteristic voltages of nodes 5, 9, and 11 are known based on the assumptions in Section 2.3. The section unit characteristic voltage drop is defined as follows:

$$U_c = \left| \frac{\Delta U_{sec}}{\Delta L} \right| \tag{4}$$

where $\Delta \boldsymbol{U}_{sec}$ represents the phasor difference of the characteristic voltage at both ends of the section and ΔL represents the impedance of this section. The fault determination indices of the three sections need to be calculated. Section 1 and Section 2 are upstream of the fault point, while Section 3 contains both upstream and downstream segments of the fault, so the indicators Uc of Section 1 and Section 2 should be approximately equal and much larger than that of Section 3. This difference indicates that the fault is in Section 3.

Figure 1 illustrates that the voltage measured at node 1 is in the medium-voltage side, while there are no low-voltage side measurement points at node 2 or node 3; therefore, the data from the low-voltage side cannot be acquired directly. The following steps should be taken: 1) The characteristic voltage of the low-voltage side at node 1 is directly calculated according to Eqs 1, 2; 2) The characteristic voltage at nodes 2 and 3 is calculated using the voltage of the measuring point at the end of the corresponding branch, and the load impedance is obtained from the voltage and current data before the fault. The voltage of node 2 is calculated based on node 9, and that of node 3 is based on the voltage of node 5 (or node 14). It should be noted that the characteristic current flowing through the nonfault path is very small during a fault. For example, the negative sequence current of the nonfault branch in a single-phase ground fault is almost zero, while the load current of the nonfault branch is much smaller than the short-circuit current of the fault branch given an interphase short-circuit fault. Therefore, the fault section can be further determined by comparing the Uc values of each section in the suspected fault path.

3.5 The measuring point configuration

In this paper, the fault section is determined according to the principle that the characteristic voltage of the fault point has the maximum value. In theory, the more measurement points there are, the greater the positioning accuracy. However, the distribution network structure is complex, there are many nodes, and a large number of measuring points leads to a substantial increase in cost. Therefore, combined with the characteristics of the location method, the following measuring point configuration principles based on the fault location of voltage measurements on the low-voltage side are determined: 1) The measurement points should be configured on the secondary side of the distribution transformer at the end of the long branch, while the short branch does not need to be installed if the positioning accuracy is satisfied. As shown in Figure 1, nodes 5, 9, 11 and 14 are all at the end of the long branch, while the branch of node 12 is so short that the measuring points cannot be set. 2) For a feeder line with no branches in a large area, to meet the location accuracy requirements, measurement points should be properly configured on the secondary side of the distribution transformers directly connected to the main line. As shown in Figure 1, the line between node 2 and node 9 has no branches. In this case, measurement points can be configured on the secondary side of the transformer directly connected to node 7 to improve the location accuracy.

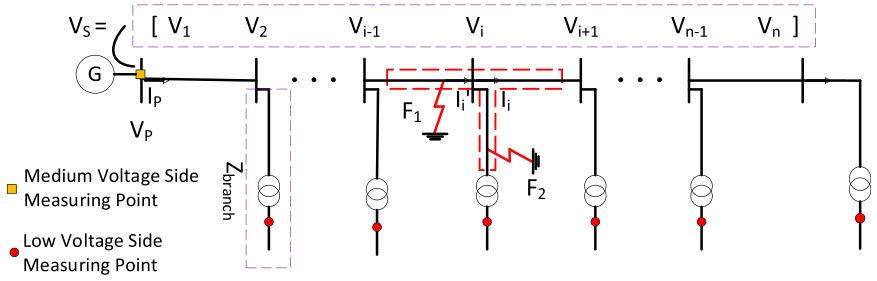

FIGURE 2
Simple distribution network topology.

4 The method of fault distance estimation

4.1 Theory of fault distance estimation

After the fault section is obtained, the characteristic voltage information and current information of both sides of the fault section and the beginning side of the branch (T node) are needed to measure the fault distance occurring in the main feeder or branch. The calculation of characteristic voltage information and current information needs to take the load current into account. This suitable for time-varying loads and different load models. First, the characteristic voltage information and current information of the two sides of the fault section are calculated by the topology parameters of the line and the measuring information of the distribution station. Then, the characteristic voltage of the fault point is calculated using the information of both sides. Finally, according to the principle that the voltages calculated from both sides are the same, the fault distance is obtained.

4.2 Calculation of fault section sides voltage

Figure 2 shows the topology of a simple distribution network. The above section shows that the characteristic voltage of a single-phase fault and two-phase fault is the negative sequence voltage, while the characteristic voltage of a three-phase fault is the phase voltage of any phase. Taking the following distribution network topology as an example, the characteristic voltage information and current information of the initial side can be obtained from the distribution station. When the main feeder or branch fails, the characteristic voltage information and current information **(VP, IP)** of the initial side can be passed without considering the fault current. The characteristic voltages of each node upstream and downstream of the fault are calculated, and the feeder node voltage matrix V_S is formed based on the voltage of the initial side.

Taking the main feeder fault F1 and branch fault F2 as examples, the line distribution parameter model is used to calculate the voltage matrix of the main feeder node point by point according to the voltage and current information of the initial side. Finally, the voltage difference matrix of each node is obtained. The calculation equations for the voltage of the main feeder node and the current flowing out of the node are shown in Eqs 5, 6, respectively.

$$\begin{bmatrix} V_i \\ I_i^{'} \end{bmatrix} = \begin{bmatrix} \cosh \gamma x_i & -Z_c \sinh \gamma x_i \\ -Z_c^{-1} \sinh \gamma x_i & \cosh \gamma x_i \end{bmatrix} \begin{bmatrix} V_{i-1} \\ I_{i-1} \end{bmatrix} \tag{5}$$

$$I_i = I_i^{'} - V_i / Z_{\text{branch}} \tag{6}$$

V_i and I_i are the voltage of node i and the current flowing out of node i, respectively, and the current flowing into the node. $\gamma = \sqrt{j\omega CR - \omega^2 LC}$ is the transmission coefficient, and $Z_c = \sqrt{(R + j\omega L)/j\omega C}$ is the characteristic impedance. x_i is the distance between node i and node i-1, and Z_{branch} is the equivalent impedance of the branch connected to the node. The characteristic voltage and current values at both sides of the fault section can be obtained by the above formulas. L and C represent the inductance and capacitance of this section of the line, respectively.

4.3 The fault distance estimation of the main feeder

Figure 3 shows the fault section on the main feeder line. Assuming that the fault occurs at the position that is x relative distance from the beginning of the section, the characteristic voltage and current at both sides of the fault section are obtained as described in the previous section, V_L、I_L、V_R、I_R, and the voltage at the fault point is calculated by using the current and voltage information at both sides. The voltage at the fault point calculated by the information from the beginning and end of the fault section $V_{FS}(x)$、$V_{FE}(x)$ can be obtained by Eqs 7, 8.

$$\begin{bmatrix} V_{FS}(x) \\ I_{\text{FS}}^{'}(x) \end{bmatrix} = \begin{bmatrix} \cosh \gamma x & -Z_c \sinh \gamma x \\ -Z_c^{-1} \sinh \gamma x & \cosh \gamma x \end{bmatrix} \begin{bmatrix} V_L \\ I_L \end{bmatrix} \tag{7}$$

$$\begin{bmatrix} V_R \\ I_R \end{bmatrix} = \begin{bmatrix} \cosh \gamma (1-x) & -Z_c \sinh \gamma (1-x) \\ -Z_c^{-1} \sinh \gamma (1-x) & \cosh \gamma (1-x) \end{bmatrix} \begin{bmatrix} V_{FE}(x) \\ I_{\text{FE}}(x) \end{bmatrix} \tag{8}$$

$I_{\text{FS}}^{'}(x)$ is the current flowing into the faulty node calculated from the information at the beginning of the section, and $I_{\text{FE}}(x)$ is the current flowing out of the faulty node calculated based on the information at the end of the segment. According to the information at the beginning and end of the fault section, the voltages of the fault points are equal, and the construction function is as follows.

$$F_M(x) = |V_{\text{Fs}}(x) - V_{\text{Fe}}(x)| \tag{9}$$

When FM(x) reaches the minimum value, the corresponding x is the actual fault distance.

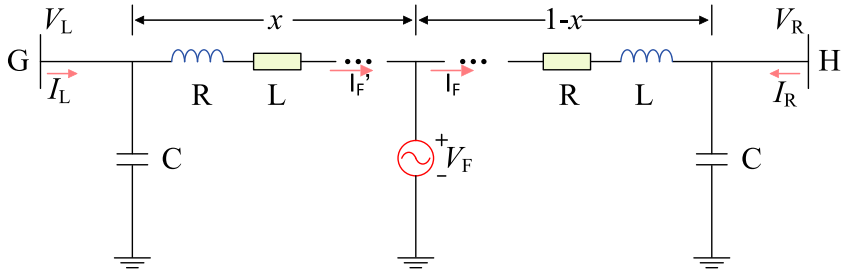

FIGURE 3
Diagram of the fault section of the main feeder.

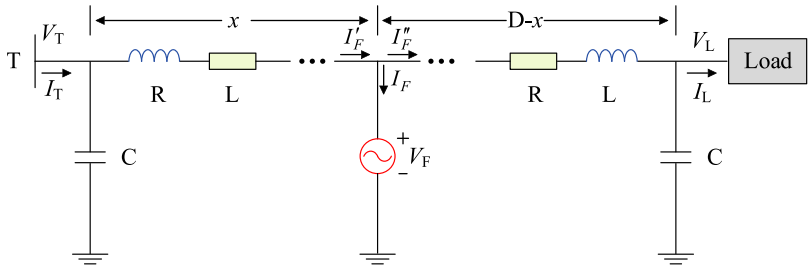

FIGURE 4
Branch fault section diagram.

4.4 Fault distance estimation of the branch

Taking the branches in Figure 4 as the research object, the line distribution parameter model is adopted to establish a single-sided fault distance estimation model. To determine the single-sided fault location by using the data of the T node, the relationship between the characteristic voltage and current at the end of the branches needs to be established.

According to the law of voltage/current propagation, the following relationship can be obtained:

$$\begin{bmatrix} V_F \\ I_F' \end{bmatrix} = \begin{bmatrix} \cosh \gamma x & -Z_c \sinh \gamma x \\ -Z_c^{-1} \sinh \gamma x & \cosh \gamma x \end{bmatrix} \begin{bmatrix} V_T \\ I_T \end{bmatrix} \tag{10}$$

$$\begin{bmatrix} V_L \\ I_L \end{bmatrix} = \begin{bmatrix} \cosh \gamma (D-x) & -Z_c \sinh \gamma (D-x) \\ -Z_c^{-1} \sinh \gamma (D-x) & \cosh \gamma (D-x) \end{bmatrix} \begin{bmatrix} V_F \\ I_F'' \end{bmatrix} \tag{11}$$

$$I_F' = I_F + I_F'' \tag{12}$$

V_T and I_T are the voltage of the T node and the current flowing into the branch, respectively; V_F and V_L are the voltage phasors of the fault point and the end of the fault branch, respectively; I_F' and I_F'' are the current phasors flowing into and out of the fault branch, respectively; and I_F and I_L are the fault current and the current flowing into the load, respectively.

5 The fault location algorithm flow

The fault section location process of the medium-voltage distribution network based on the characteristic voltage of the low-voltage side is shown in Figure 5. The specific process is as follows:

1) Determination of the characteristic voltage. In this paper, the scheme proposed in reference (Arsoniadis et al., 2021) is adopted to identify fault types, and the corresponding characteristic voltage is selected according to the determination principle of the characteristic voltage in Table 2.
2) Identification of suspected fault paths. The characteristic voltage at each measuring point is calculated, and the measuring point where the maximum characteristic voltage is located is determined. The suspected fault path is the shortest path between the power point and the measurement point or the shortest path between the common nodes of multiple measurement points.
3) Performance of the fault section search algorithm and fault section determination. The suspicious fault path is segmented by each branch measuring point, and the numbers are sorted from the system power supply side. The fault determination index Uc of each section is calculated by the characteristic voltage phasor difference between the two sides of the section, and the fault section is determined by comparing the Uc values corresponding to each section.
4) The characteristic voltage of each node upstream and downstream of the fault is calculated by the characteristic voltage information and current information of the distribution station, and the feeder node voltage matrix V_S based on the voltage of the distribution station is formed. The characteristic voltage and current at both sides of the fault section are derived, and the characteristic voltage at the fault point is subsequently derived from the first and end of the fault section to determine the corresponding position when the voltage is equal.

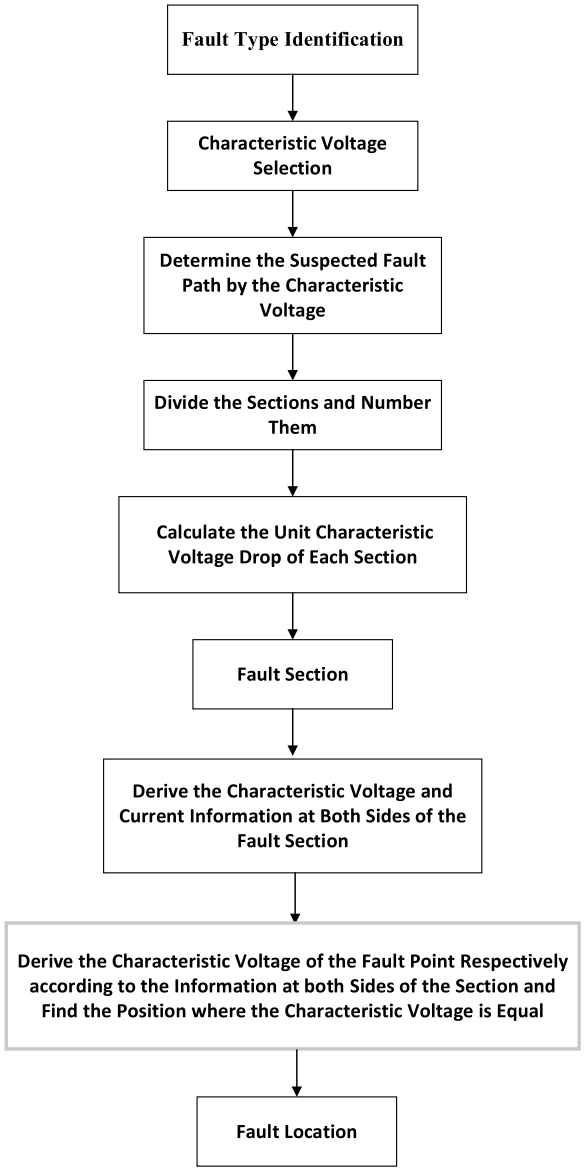

FIGURE 5
Flowchart of fault segment location.

6 Simulation and verification

A model of an actual 10 kV distribution network in Guangdong Province is built using the PSCAD/EMTDC platform. The system structure topology diagram is shown in Figure 6. Following the analysis in Section 3.5, voltage measuring devices are configured on the reference power outlet nodes and the low-voltage side of the end nodes of the distribution network. The positions of the measuring points on the low-voltage side are shown by the red dots in Figure 6.

Now, the single-phase metallic ground fault between nodes #26 and #27 and 250 m away from node #27 are taken as an example to describe how to locate fault sections. Taking the three-phase voltage at each measuring point after the fault, the negative sequence component is selected as the characteristic voltage, and the negative sequence voltage at each measuring point is calculated separately, as shown in Figure 7. The negative sequence component of measuring point 18 is the largest, so the suspected fault path is determined as shown in the dotted line box in Figure 6. The section is divided into 3 subsections by branch with measuring points.

The unit characteristic voltage drop Uc of each section is calculated separately, and the Uc values of all sections are displayed in the same dimension to clearly distinguish the fault section from the rest of the section. As shown in Figure 8, the green points with larger amplitudes are indicators of upstream fault sections #20-#25 and #10-#20, the red points with the smallest amplitude are indicators of sections #25-#27, and the fault section is consistent with the preset fault position. It should be noted that in some cases, the suspected fault path determined by the characteristic voltage does not include the section completely downstream of the fault but rather only the Uc upstream of the fault and fault section. Finally, the fault is accurately located, the positioning result is 12757.37 m, and the error is only 7.37 m.

1) Effect of the fault resistance

Fault resistance may affect the value of the negative sequence component in a single-phase grounding fault, thereby affecting the location effect of a single-phase grounding fault. However, in the case of phase-to-phase, two-phase ground and three-phase ground faults, the corresponding phase voltage on the low-voltage side of the fault point is always zero. That is, the fault resistance does not affect the distribution of the corresponding phase voltage on the low-voltage side because the line voltage distribution of the two-fault phase on the medium-voltage side always drops from the station terminal rating value to zero at the fault point, and the distribution is related only to the faulty line. Therefore, in this section, only the effect of fault resistance on the single-phase grounding location is discussed. Now, the single-phase grounding fault between nodes #26 and #27 and 250 m away from node #27 is taken as an example, and the fault section is located under different fault resistances, fault segments can still be accurately obtained according to Uc when the fault resistance increases to 3,000 Ω. Therefore, the proposed method is not affected by the fault resistance. Then, fault location estimation is performed for different fault resistances, and the results are obtained, as shown in Table 3. When the fault resistance increases to 3,000 Ω, the positioning error remains within an acceptable range.

2) Effect of the Fault Position

To verify the accuracy and effectiveness of this method on the entire network, a single-phase ground fault is used as an example, and faults with no fault resistance are simulated at different positions in the distribution network. The specific fault positions are as follows:

F1: between node #126 and node #127, 250 m away from node #127.

F2: between node #3 and node #4, 250 m away from node #4.

F3: between node #26 and node #27, 250 m away from node #27.

F4: between node #21 and node #49, 250 m away from node #49.

F5: between node #164 and node #1, 250 m away from node #1.

The suspected fault segments are shown in the dotted line box in Figure 6.

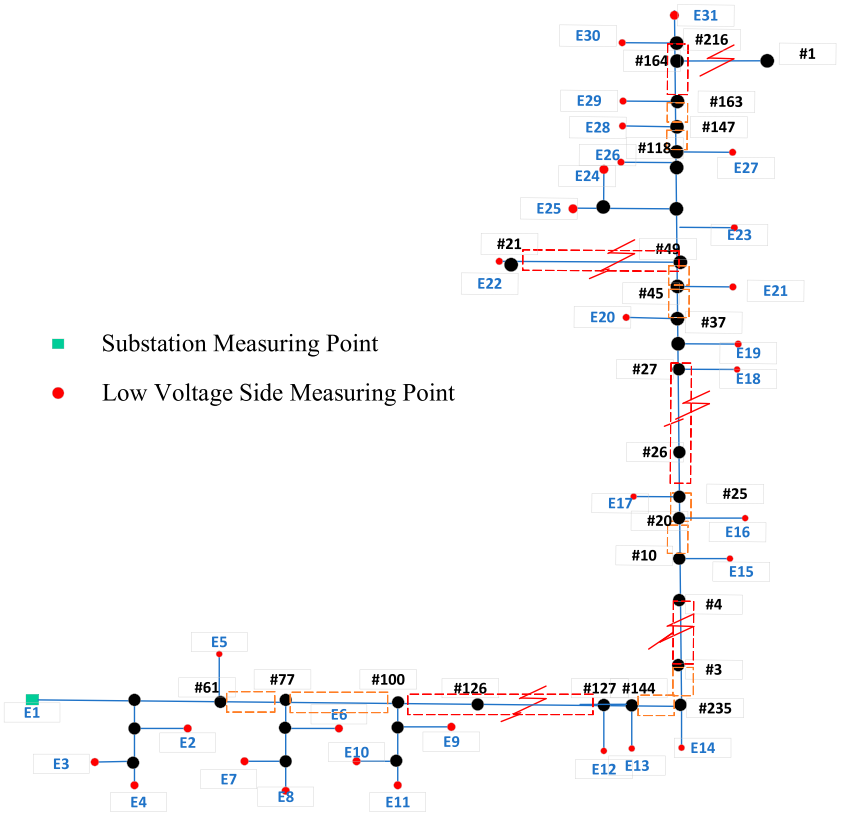

FIGURE 6
Topology of an actual distribution network in Guangdong Province.

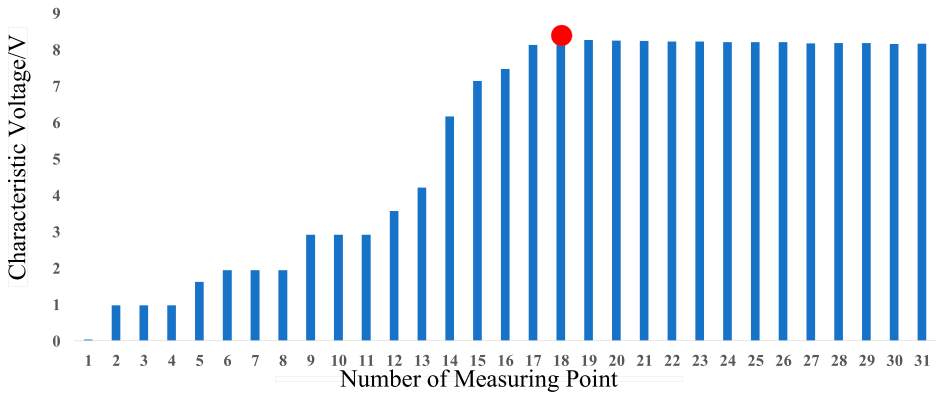

FIGURE 7
Characteristic voltage of a single-phase ground fault.

When the fault is located in the main feeder line, the characteristic voltages of multiple measuring points downstream of the fault reach the maximum value. When the fault is located in the branch, only the characteristic voltage of the branch reaches the maximum value. That is, the number of measuring points with the maximum value of the characteristic voltage is related to the fault location. The fault location results illustrate that the scheme can accurately distinguish the fault section from the nonfault section at each fault location, and the results are consistent with the preset fault positions. Therefore, this method can determine the section location under each fault position.

Then, the fault distance is estimated for each position. The results are shown in Table 4, indicating that the location is not affected by the fault location.

3) Effect of the Fault Type

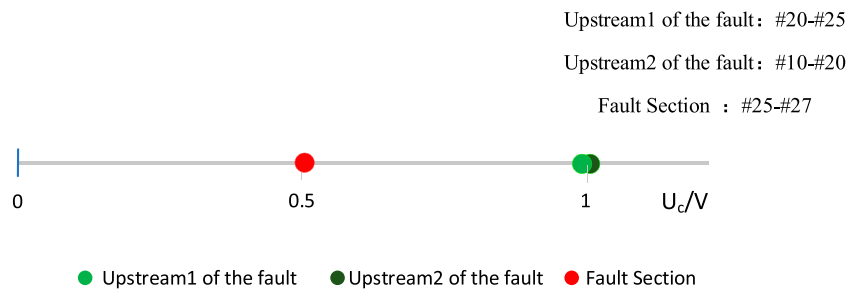

FIGURE 8
Location result of single-phase grounding fault.

TABLE 3 Fault distance estimation results under different fault resistors.

Fault resistance/ohms	Actual fault location/m	Estimated fault location/m	Absolute Error/m	Relative error
0	12,750	12757.37	7.37	5.78E-04
10	12,750	12753.54	3.54	2.78E-04
50	12,750	12738.01	11.99	9.40E-04
100	12,750	12719.79	31.21	2.45E-03
500	12,750	12627.01	122.99	9.65E-03
3,000	12,750	12531.99	218.01	1.71E-02

TABLE 4 Fault distance estimation results under different fault locations.

Actual fault location/m	Estimated fault location/m	Absolute Error/m	Relative error
5,250	5236.03	13.97	2.66E-03
10,250	10260.56	10.56	1.03E-03
12,750	12757.37	7.37	5.78E-04
16,750	16800.79	50.79	3.03E-03
25,750	25690.40	59.60	2.31E-03

To verify the applicability of the method to all types of faults, different types of faults are simulated between nodes #26 and #27, 250 m away from node #27, and the fault resistance is set to zero, the proposed method is not affected by the fault type. The fault distance is estimated, and the results are shown in Table 5. These results indicate that the algorithm is not affected by the fault type.

4) Effect of the System Neutral Grounding Mode

The grounding mode of the system affects the variation range of the fault voltage and even determines the presence or absence of this component. For an ungrounded system, if the line-to-ground capacitance is ignored, there is no negative sequence or zero-sequence component on the low-voltage side when a single-phase grounding fault occurs, which affects the positioning result. The fault position is between node #26 and node #27, 250 m away from node #27, the system grounding mode has no effect on the location results of the phase-to-phase fault, two-phase ground fault or three-phase ground fault. The velocity is determined by the line voltage amplitude between the two fault phase distributions from the station terminal to the fault point. The location result is related only to the fault distance. For a single-phase grounding fault, with increasing zero-sequence impedance, the negative-sequence component decreases, but this does not affect the positioning result.

Then, a single-phase grounding fault is taken as an example. The fault distance is estimated under different neutral grounding modes. The location results are shown in Table 6.

5) Effect of Equipment Measurement Error

Due to environmental interference and the measurement error of the device itself, the measurement device generally introduces an error of no more than 0.5%. The existence of branches in the distribution network leads to the formation of many T-nodes.

When the fault position is near the upstream T-node, the characteristic voltage amplitudes at the two sides of the fault section are also very close. The equipment measurement error may lead to an error in determining the measurement point with

TABLE 5 Fault distance estimation results under different fault types.

Fault type	Actual fault location/m	Estimated fault location/m	Absolute Error/m	Relative error
LG	12,750	12757.37	7.37	5.78E-04
LL	12,750	12756.21	6.21	4.87E-04
LLG	12,750	12746.01	3.99	3.13E-04
LLL	12,750	12748.14	1.86	1.46E-04

TABLE 6 Fault distance estimation results under different grounding methods.

Neutral grounding mode	Actual fault location/m	Estimated fault location/m	Absolute Error/m	Relative error
Direct Grounding	12,750	12761.51	11.51	9.03E-04
Small Resistance Grounding	12,750	12757.37	7.37	5.78E-04
Ungrounding	12,750	12746.99	3.01	2.36E-04
Resonant Grounding	12,750	12745.16	4.84	3.80E-04

TABLE 7 Fault distance estimation results under different measurement errors.

Measuring error (%)	Actual fault location/m	Estimated fault location/m	Absolute Error/m	Relative error
2	12,750	12755.55	5.55	4.35E-04
−2	12,750	12756.43	6.43	5.04E-04
3	12,750	12773.66	23.66	1.86E-03
−3	12,750	12755.76	5.76	4.52E-04
4	12,750	12778.45	28.45	2.23E-03
−4	12,750	12777.26	27.36	2.15E-03

the maximum characteristic voltage. As a result, the fault is located in adjacent areas.

For example, when a single-phase grounding fault occurs, the fault resistance is set to 10 Ω. The measurement errors are introduced randomly into each measurement point, and the robustness of the positioning method to the measurement errors is discussed. Under different measurement errors, the proposed method can obtain a good section position result while considering the measurement error of the equipment. The fault distance is also estimated under different measurement errors, and the results are shown in Table 7.

7 Conclusion

The fault location method based on the measurement of the medium-voltage side has problems, such as high installation costs and difficult maintenance. In this paper, an economical and practical fault section method and a fault distance estimation method based on the characteristic voltage of the low-voltage side are proposed to solve these problems. The following conclusions can be drawn from an actual topology simulation of the distribution network in Guangdong Province.

(1) For different types of medium-voltage faults, the variation characteristics of different voltages on the low-voltage side are not the same. The characteristic voltage of a single-phase ground fault is the negative sequence voltage, the characteristic voltage of a two-phase fault is the phase voltage or the line voltage between faults, and the characteristic voltage of a three-phase fault is the phase voltage of any phase. The characteristic voltage of a single-phase grounding fault reaches its maximum value at the fault point, while the characteristic voltages of other types of faults reach their minimum value at the fault point. Downstream of the fault, the characteristic voltage amplitude is similar to that at the fault point. The suspected fault path can be determined by using the characteristic voltage of the low-voltage side.

(2) According to the difference in the characteristic voltage drop per unit distance in the upstream, fault section and fault downstream lines, the fault section in the suspected fault path is searched. An actual distribution network example in Guangdong Province shows that the proposed method is suitable for different fault resistances, fault positions, fault types and neutral ground modes. In addition, when considering measurement errors, the proposed method can also obtain good results in terms of section location and fault distance estimation.

(3) Based on the characteristic voltage of the low-voltage side, the fault section of the medium-voltage line can be located without the measurement information of the medium-voltage side. This idea is expected to be combined with the power information

acquisition system, smart metres and other measuring equipment, which have been widely used on the low-voltage side to locate faults in medium-voltage lines in distribution networks. Moreover, fault location methods based on medium-voltage side measurements (such as distribution automation and fault indicators) can be effectively applied.

(4) There are still limitations to this method and further exploration is needed. The fault location method proposed in this paper depends on the fault line parameters of distribution network. However, due to the time-varying parameters of distribution network and the inaccurate statistics, it is often difficult to accurately locate faults. Therefore, it is the future research direction to propose a fault location method independent of line parameters.

Data availability statement

The original contributions presented in the study are included in the article/Supplementary material, further inquiries can be directed to the corresponding author.

Author contributions

CH: Writing–original draft, Writing–review and editing. HH: Conceptualization, Investigation, Writing–original draft. YW: Investigation, Software, Writing–original draft. RM: Methodology, Supervision, Writing–review and editing. ZK: Conceptualization, Data curation, Investigation, Writing–review and editing. KC: Conceptualization, Investigation, Writing–original draft.

Funding

The author(s) declare financial support was received for the research, authorship, and/or publication of this article. China Southern Power Grid technology project (030800KK52220015).

Conflict of interest

Authors CH, HH, YW, RM, ZK, and CK were employed by Zhanjiang Power Supply Bureau of Guangdong Power Grid Co., Ltd.

Publisher's note

All claims expressed in this article are solely those of the authors and do not necessarily represent those of their affiliated organizations, or those of the publisher, the editors and the reviewers. Any product that may be evaluated in this article, or claim that may be made by its manufacturer, is not guaranteed or endorsed by the publisher.

References

Alwash, S. F., Ramachandaramurthy, V. K., and Mithulananthan, N. (2015). Fault-location scheme for power distribution system with distributed generation. *IEEE Trans. Power Deliv.* 30 (3), 1187–1195. doi:10.1109/tpwrd.2014.2372045

Arsoniadis, C., Apostolopoulos, C., Georgilakis, P., and Nikolaidis, V. C. (2021). A voltage-based fault location algorithm for medium voltage active distribution systems. *Electr. Power Syst. Res.* 196, 107236. doi:10.1016/j.epsr.2021.107236

Bingyin, X. U., Tianyou, L. I., and Yongduan, X. U. E. (2017). *Relay protection and automation of distribution network[M]*. Beijing, China: China Electric Power Press.

Buzo, R., Barradas, H., and Leão, F. (2021). A new method for fault location in distribution networks based on voltage sag measurements. *IEEE Trans. Power Deliv.* 36 (2), 651–662. doi:10.1109/tpwrd.2020.2987892

Conte, F., D'Agostino, F., Gabriele, B., Schiapparelli, G. P., and Silvestro, F. (2023). Fault detection and localization in active distribution networks using optimally placed phasor measurements units. *IEEE Trans. Power Syst.* 38 (1), 714–727. doi:10.1109/tpwrs.2022.3165685

Crespo, D., and Moreto, M. (2022). New technique for fault location in distribution systems using sincrophasor voltages. *Electr. Power Syst. Res.* 212, 108485. doi:10.1016/j.epsr.2022.108485

Dashtdar, M., Hussain, A., Al Garni, H., Mas'ud, A. A., Haider, W., AboRas, K. M., et al. (2023). Fault location in distribution network by solving the optimization problem based on power system status estimation using the PMU. *Machines* 11 (1), 109. doi:10.3390/machines11010109

Dobakhshari, A. S. (2018). Wide-area Fault Location of transmission lines by hybrid synchronized/unsynchronized voltage measurements. *IEEE Trans. Smart Grid* 9 (3), 1–1877. doi:10.1109/tsg.2016.2601379

Dobakhshari, A. S., and Ranjbar, A. M. (2015). A wide-area scheme for power system Fault Location incorporating bad data detection. *IEEE Trans. Power Deliv.* 30 (2), 800–808. doi:10.1109/tpwrd.2014.2352336

Feng, DENG, Yarui, Z. U., Huang, Y., Zeng, X., Li, Z., Xu, F., et al. (2021). Research on single-ended positioning method based on main frequency component of traveling wave full waveform. *Proc. CSEE* 41 (06), 2156–2168.

Feng, DENG, Zeng, X., Ma, S., Zhao, D., et al. (2017). Fault location method for wide area network based on distributed traveling wave detection. *Power Syst. Technol.* 41 (04), 1300–1310.

Feng, G., and Abur, A. (2016). Fault location using wide-area measurements and sparse estimation. *IEEE Trans. Power Syst.* 31 (4), 2938–2945. doi:10.1109/tpwrs.2015.2469606

Gabr, M. A., Ibrahim, D. K., Ahmed, E. S., and Gilany, M. I. (2017). A new impedance-based fault location scheme for overhead unbalanced radial distribution networks. *Electr. Power Syst. Res.* 142, 153–162. doi:10.1016/j.epsr.2016.09.015

Ge, W., Zhang, S., Zhang, Y., Li, T., Li, J., Gao, F., et al. (2020). Distribution network fault location method based on μPMU synchronous measurement data. *Power Syst. Prot. Control* 48 (04), 39–46.

Jia, Ke, Dong, X., Li, L., Feng, T., and Bi, T. (2020). Fault location of distribution network based on sparse voltage amplitude measurement. *Power Syst. Technol.* 44 (03), 835–845.

Jia, Ke, Li, L., Yang, Z., Zhao, G., and Bi, T. (2019). Research on distribution network fault location based on Bayesian compressed sensing theory. *Proc. CSEE* 39 (12), 3475–3486.

Jia, K., Ren, Z., Bi, T., and Yang, Q. (2015). Ground Fault location using the low-voltage-side recorded data in distribution systems. *IEEE Trans. Industry Appl.* 51 (6), 4994–5001. doi:10.1109/tia.2015.2425358

Li, J., Gao, M., Liu, B., Gao, F., and Chen, J. (2021). Fault location algorithm in distribution networks considering distributed capacitive current. *IEEE Trans. Power Deliv.* 36 (5), 2785–2793. doi:10.1109/tpwrd.2020.3026835

Li, Y. U., Zaibin, JIAO, Xiaopeng, WANG, Li, S., Wang, R., Yang, L., et al. (2020). Quantitative analysis of differentially expressed proteins in psoriasis vulgaris using tandem mass tags and parallel reaction monitoring. *Automation Electr. Power Syst.* 44 (18), 30–38. doi:10.1186/s12014-020-09293-8

Lotfifard, S., Kezunovic, M., and Mousavi, M. J. (2011). Voltage sag data utilization for distribution Fault Location. *IEEE Trans. Power Deliv.* 26 (2), 1239–1246. doi:10.1109/tpwrd.2010.2098891

Lu, J., Luo, Y., Zhong, L., Gan, H., et al. (2016). New fault location algorithm based on longitudinal impedance. *High. Volt. Eng.* 42 (02), 605–611.

Penido, D., de Araujo, L., Rodrigues, V., and do Nascimento, K. B. (2022). An analytical zero sequence method to locate fault in distribution systems rich in DG. *IEEE Trans. Smart Grid* 13 (3), 1849–1859. doi:10.1109/tsg.2022.3141207

Rong, G. U. O., Xindong, L. I. U., and Zeng, R. (2013). Research on Fault Location algorithm of high voltage long line with shunt reactor. *Mod. Electr. Power* 30 (04), 62–66.

Rui, LIANG, Lianhua, C. U. I., Zhili, D. U., Li, G., Fu, G., et al. (2014). Fault line selection and location of distribution network based on the time difference relation matrix of the initial wave head of wide area traveling wave. *High. Volt. Eng.* 40 (11), 3411–3417.

Shichao, M. A., and Liu, Y. (2010). Simulation research of cable fault traveling wave location based on wavelet analysis. *Mod. Electr. Power* 27 (06), 16–20.

Sun, H., Yi, H., Zhuo, F., Du, X., and Yang, G. (2020). Precise Fault location in distribution networks based on optimal monitor allocation. *IEEE Trans. Power Deliv.* 35 (4), 1788–1799. doi:10.1109/tpwrd.2019.2954460

Tashakkori, A., Abu-Siada, A., Wolfs, P. J., and Islam, S. (2021). Optimal placement of synchronized voltage traveling wave sensors in a radial distribution network. *IEEE Access* 9, 65380–65387. doi:10.1109/access.2021.3076465

Trindade, F. C. L., and Freitas, W. (2017). Low voltage zones to support Fault Location in distribution systems with smart meters. *IEEE Trans. Smart Grid* 8 (6), 2765–2774. doi:10.1109/tsg.2016.2538268

Trindade, F. C. L., Freitas, W., and Vieira, J. C. M. (2014). Fault location in distribution systems based on smart feeder meters. *IEEE Trans. Power Deliv.* 29 (1), 251–260. doi:10.1109/tpwrd.2013.2272057

Xu, B., Xue, Y., Feng, G., and Wang, C. (2019). Discussion on several problems of earth-fault protection in distribution network. *Automation Electr. Power Syst.* 43 (20), 1–7.

Yan, V. T., Fernandes, R., and Coury, D. V. (2021). Reducing multiple estimation for fault location in medium voltage distribution networks. *Electr. Power Syst. Res.* 199, 107424. doi:10.1016/j.epsr.2021.107424

Yang, B., Jia, K., Liu, Q., Zheng, L., and Bi, T. (2022). Faulted line-section location in distribution system with inverter-interfaced DGs using sparse meters. *IEEE Trans. Smart Grid* 14 (1), 413–423. doi:10.1109/tsg.2022.3186541

Yang, R., Gao, H., and Liu, J. (2022). Distribution network fault location based on limited PMU configuration. *Electr. Power Autom. Equip.* 42 (04), 138–145.

Zhang, J., Gao, Z., Wang, Z., Sun, X., and Zhang, S. (2020). Fault location method for active distribution network based on finite μPMU. *Power Syst. Technol.* 44 (07), 2722–2731.